Turbulent Compressible Flow in a Slender Tube

Kurt O. Lund*[1], and Christine M. Lord [2]
[1]COMSOL Consultant, [2]Lord Engineering Corp.
*Corresponding author: 135 Sixth Street, Del Mar, CA 92014, kurtlund@roadrunner.com

Abstract: Pressure-drop experiments were conducted for the turbulent, compressible flow of air in a small, slender tube, and modeled with COMSOL heat transfer module, and analytically. A scalar integration variable is introduced which integrates the mass velocity [kg/m^{2}s] over the inlet area and iteratively equates this to the input mass flow [kg/s]. For computation, the temperature specification is related to the local, calculated pressure through the isentropic relationships. Additionally, based on the numerical results, an analytical 1-D model is derived. The results show significant density variations along the tube, and indicate choking at the outlet (Ma ~ 1) for the highest flow. For the adiabatic conditions, there is excellent agreement with the experimental data for a wide range of flows, though excluding near-choking conditions at the outlet.
Keywords: compressible air-flow, COMSOL scalar integration variable, experimental data, analytical approximation, specified mass flow.

1. Introduction

The compressible flow of gases at elevated temperatures and pressures is important in many industrial applications. However, it is impractical to conduct experiments at the application conditions; therefore, "scale-up" of experimental results in atmospheric air to other gases at higher temperatures and pressures requires numerical modeling. Although numerical modeling can be done directly, experimental verification is important to assure accuracy. Usually, process applications are specified in terms of mass flow [kg/h]; hence, the experimental measurements are scaled for the mass flow of air.

In this paper, the air-flow experiment is described, and COMSOL heat transfer module is used with the k-ε turbulence theory to model the axis-symmetric flow and pressure fields. Additionally, based on the numerical results, an analytical 1-D model is derived.

The usual boundary conditions for flow simulation are specified pressure at the outlet (here atmospheric), and velocity at the inlet; however, for inlet condition specified as mass flow, the unknown pressure at the inlet is needed to determine the velocity. Therefore, a scalar integration variable is introduced which integrates the mass velocity [kg/m^{2}s] over the inlet area and iteratively equates this to the specified mass flow, mdot[kg/s].

For computation, the COMSOL built-in library properties for air were used initially, which, with a constant temperature, resulted in the isothermal compression of the flow. However, the high-velocity air-flow is closer to adiabatic conditions; thus, the temperature specification was related to the local, calculated pressure through the isentropic relationships.

The results of the COMSOL computation show significant density variation along the tube, and indicate choking at the outlet (Ma ~ 1) for the highest flow. For the adiabatic conditions, there is excellent agreement with the experimental data for a wide range of flows, though excluding near-choking conditions at the outlet for the highest flow case.

2. Experimental Approach

In order to determine the pressure drop across the test piece, compressed air was forced through the slender tube via a flexible hose, using a rotameter and pressure gauge for the measurements, as shown in Fig. 1 below:

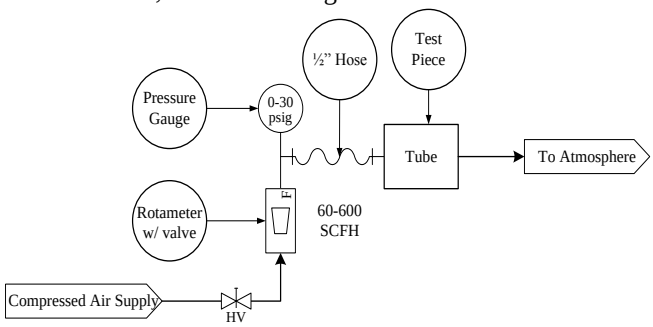

Figure 1: Test Setup

To correct for the pressure loss in the hose and fittings, a test was also run without the tube

(test section) connected. In this way, when the comparative pressures are subtracted, the pressure drop for the test section, only, is obtained.

Using a rotameter [60-600 SCFH+/-12 (2%)] and digital pressure gauge [0-30psig+/-0.3psi (1%)], tests were conducted from 100-400 SCFH by 50 SCFH increments and pressures recorded; tests with these conditions were repeated without the test section installed.

The observed rotameter readings were corrected for pressure using equation (1a):

$$Q_2 = Q_1 \times \sqrt{\frac{P_1}{P_2}} \tag{1a}$$

where:

Q_1= observed flow meter reading;
Q_2= standard flow corrected for pressure;
P_1= observed absolute pressure;
P_2= standard absolute pressure (1 atm);

These corrected volumetric flows were then converted to kg/hr using equation (1b):

$$Q_2\left[\frac{kg}{hr}\right] = Q_2\left[SCFH\right] \times \rho_2\left[\frac{kg}{ft^3}\right] \tag{1b}$$

where ρ_2 = is the density [kg/ft^3] at 70^{O}F and 14.7 psia [0.03397 kg/ft^3].

The pressure drop across the slender tube, only, was then calculated by subtracting the empty hose pressure drop:

$$P_{Tube} = P_{Total} - P_{Empty} \tag{1c}$$

Typically, in applications, it is the mass flow that is specified [kg/hr], rather than the volumetric flow; therefore, the above corrections were made. The results are in the Appendix.

3. Use of COMSOL Multiphysics

The axis-symmetric turbulent flow of air in a 4.2mm x 150mm tube, having inlet and outlet plena, was modeled with COMSOL. This geometry is shown in Fig. 2, where the flow is from left to right, with U_{in} as the plenum inlet velocity.

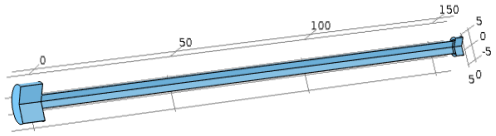

Figure 2. COMSOL Axis-symmetric Geometry

The inlet plenum matches the experimental geometry, including a small radius at the tube-entrance corner; although quite small, the fillet had an important smoothing effect on the flow development and pressure drop, as indicated by the streamlines in Fig. 3.

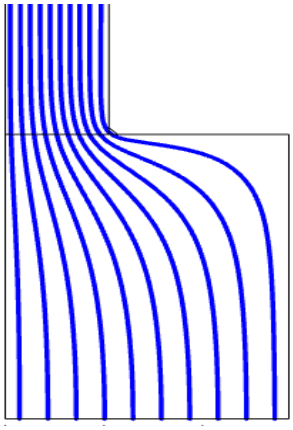

Figure 3. Inlet Streamlines

The inlet velocity is computed from a scalar integration variable, as shown in Fig. 4:

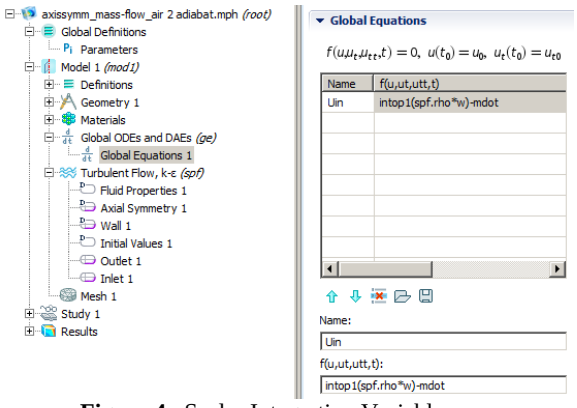

Figure 4. Scalar Integration Variable

This shows that *Uin* is to be selected (by COMSOL) such that the function *intop1(spf.rho*w)-mdot = 0*; or, in other words, such that the integration operator 1 integrates the computed mass velocity $\rho \cdot w$ over the inlet area and iteratively sets the value to the specified mass flow rate, *mdot*. Although this procedure is automatic in the CFD module, it was not available in the Heat Transfer module at this writing.

There is another important feature of the model: because the rapid, compressible flow is adiabatic, the temperature and density along the tube varies. Thus, the variables must be set as shown in Fig. 5, where p is the calculated pressure:

Variables

Name	Expression	Unit	Description
gam	1.4		Cp/Cv
T	Tin*(p/pin)^((gam-1)/gam)	K	Temperature
rho	p/(Rgas*T)	kg/m³	Density
c	sqrt(gam*Rgas*T)	m/s	Speed of Sound
Ma	w/c		Mach number

Figure 5. Setting of Variables.

With the scalar integration process in place, the inlet mass flow can be specified; thus, at a mass flow rate of 10 kg/h, the velocities appear as in Fig 6:

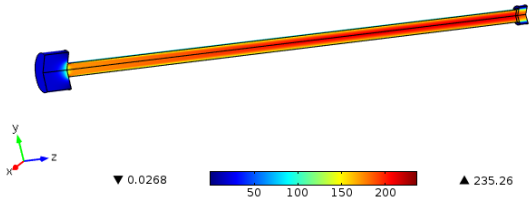

Figure 6. Velocity Distribution at 10 kg/h.

At the inlet, there are smooth flow and boundary layer developments, shown in Fig. 7 for 10 kg/h:

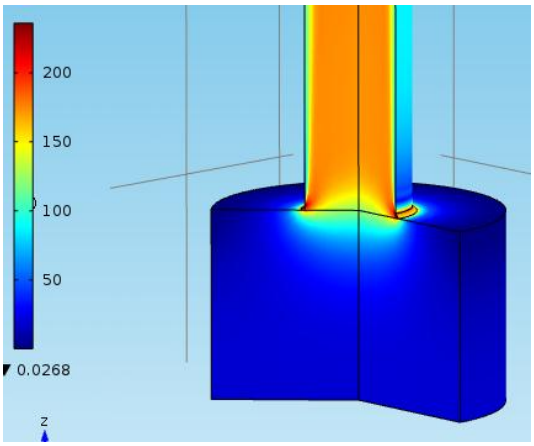

Figure 7. Inlet Flow Distribution.

It is seen that at this mass flow, there is substantial velocity of ~200 m/s in the tube. There is also substantial pressure conversion, as shown by the gauge pressures in Fig. 8:

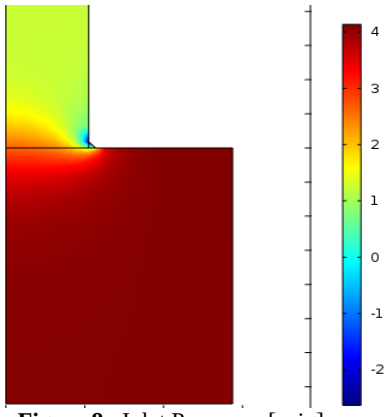

Figure 8. Inlet Pressures [psig].

At the outlet there is flow separation, and pressure recovery, shown in Figs. 9 and 10:

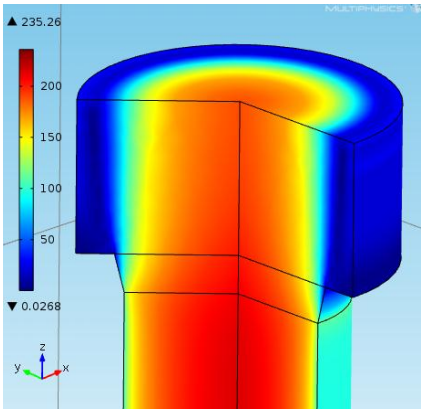

Figure 9. Outlet Flow Distribution.

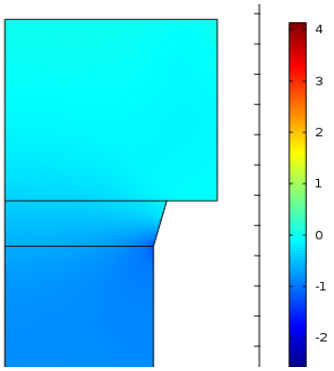

Figure 10. Pressure Recovery at Outlet.

In summary, the axial pressure profiles for four mass flows, 5 - 20 kg/h, are as shown in Fig. 11:

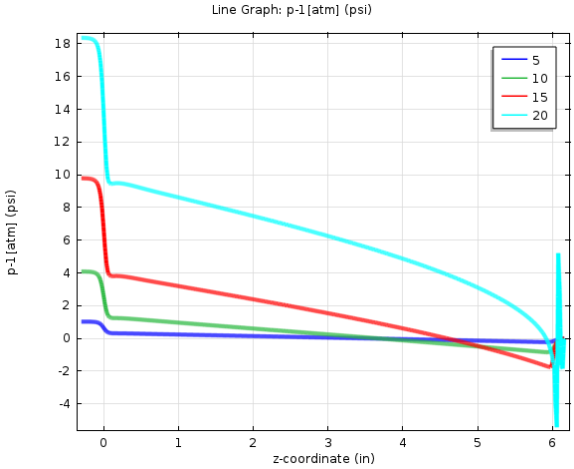

Figure 11. Pressures for mdot = 5 to 20 kg/h.

The highest flow (light green curve) shows instability at the outlet because of choking conditions. The curvature is the result of flow acceleration due to density variations.

4. Comparison of Results.

In Fig. 12 is shown the overall pressures. It is seen that there is excellent agreement between experiment and computation at the lower flows, which emphasizes the accuracy of the experimental approach, and of the applicability of the k-ε turbulence model. At the higher flows, the flow is becoming choked at the outlet, and the mildly-compressible COMSOL model is strictly not applicable; additionally some experimental error may be present for this case.

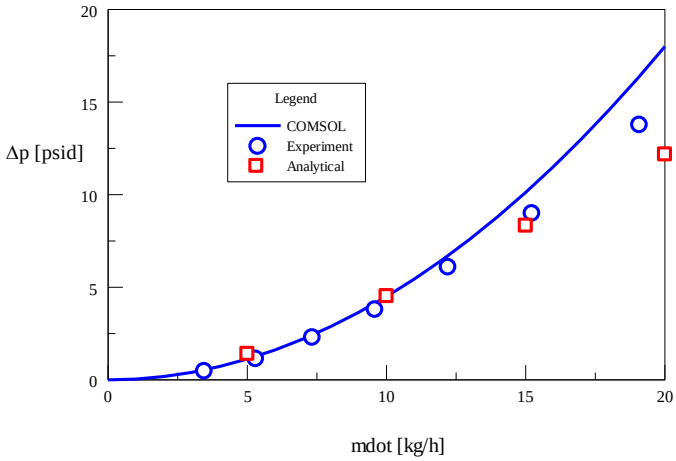

Figure 12. Overall Pressure Drop Results.

(the analytical data are discussed subsequently).

The exit flows are illustrated here for 15 kg/h

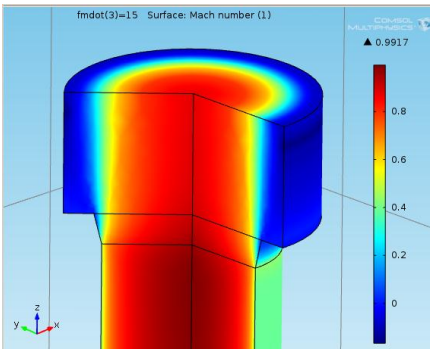

Figure 13. Exit Flow at 15 kg/h.

and for the choked condition at 20 kg/h

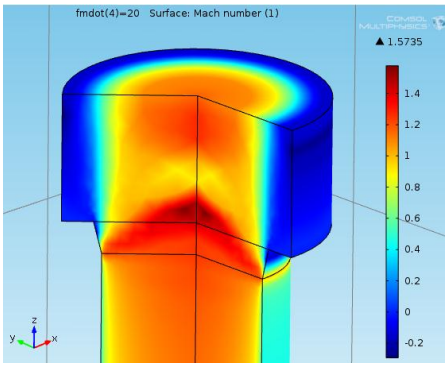

Figure 14. Exit Flow at 20 kg/h.

It is seen that the core velocity at 15 kg/h is at Ma = 1, and that this condition is exceeded at

20 kg/h; the latter exhibits the "diamond" patterns associated with supersonic nozzles.

5. One-dimensional Theory.

Considering an axial element of fluid, the pressure gradient is stated as in (2a):

$$-\frac{dp}{dx} = \frac{1}{2}\rho V^2 f\frac{1}{D} = \frac{G^2}{2\rho}\frac{f}{D} \tag{2a}$$

Where G = mdot/A is the (constant) mass velocity, and f = $0.3164/Re^{0.25}$ is the Blasius friction formula for smooth walls. Here, Re = GD/μ; except for the viscosity, the Reynolds number and friction factor are also constant along the length. The adiabatic compression relation between the pressure and density are as follows:

$$\frac{p}{p_0} = \left(\frac{\rho}{\rho_0}\right)^{\gamma} \tag{2b}$$

where subscript 0 denotes a reference value, which can be taken as the approximate inlet conditions. Thus, (2a) is written as

$$-\frac{\rho}{\rho_0}\frac{d(\frac{p}{p_0})}{dx} = -\left(\frac{p}{p_0}\right)^{1/\gamma}\frac{d(\frac{p}{p_0})}{dx} = \frac{G^2}{2\rho_0 p_0}\frac{f}{D} = const \tag{2c}$$

The integration of (2c) over δ < x < L, where δ is a short distance from the inlet, yields

$$-\left(\frac{p_L}{p_0}\right)^{\frac{\gamma-1}{\gamma}} + \left(\frac{p_\delta}{p_0}\right)^{\frac{\gamma-1}{\gamma}} = \frac{\gamma-1}{\gamma}\frac{G^2}{2\rho_0 p_0} f\frac{L-\delta}{D} \tag{3a}$$

However, these exponential pressure ratios are just the adiabatic temperature ratios; thus, (3a) is

$$-\frac{T_L}{T_0} + \frac{T_\delta}{T_0} = \frac{\gamma-1}{\gamma}\frac{G^2}{2\rho_0^2 R T_0} f\frac{L-\delta}{D} \tag{3b}$$

Hence, the adiabatic temperature at location L is

$$T_L = T_\delta - \frac{\gamma-1}{\gamma}\frac{V_0^2}{2R} f\frac{L-\delta}{D} = T_\delta - \frac{1}{2}\frac{\rho_0 V_0^2}{\rho_0 C_p} f\frac{L-\delta}{D} \tag{3c}$$

Where $V_0 = G/\rho_0$ and a ρ_0 was factored in for convenience. Once the temperature at x = L is determined, the pressure is obtained from $p_L = p_0(T_L/T_0)^{\gamma/(\gamma-1)}$, and the friction pressure loss as follows: $\Delta p_f = p_\delta - p_L$, where p_δ is the pressure after the inlet acceleration loss.

The pressure curves from COMSOL (Fig. 11) shows the (mostly) linear friction part in the center, the acceleration pressure drop at the inlet, and the pressure recovery at the outlet. Hence, the recovery at the exit is stated as

$$\Delta p_{ex} = p_L - p_{out} = \frac{1}{2}\rho_L V_L^2 (K_{ex} - 1) = \frac{G^2}{2\rho_L}(K_{ex} - 1) \tag{4a}$$

where there is conversion of 1 velocity head; Similarly, for the inlet (where a conversion is included in K_{in}):

$$\Delta p_{in} = p_{in} - p_\delta = \frac{1}{2}\rho_\delta V_\delta^2 K_{in} \approx \frac{G^2}{2\rho_{in}} K_{in} \tag{4b}$$

By comparison with the COMSOL data for 15 kg/h, as shown in Fig. 11, the inlet and outlet head-loss coefficients are determined as K_{in} = 1 (conversion) + 0.70 and K_{out} = 0.65. Keeping these values fixed, and determining the friction losses by the Blasius formula, the pressure drop data are as shown by the red squares in Fig. 12. It is seen that there is good agreement, except for the highest, choked flow rate.

6. Conclusions

Careful experiments and COMSOL modeling were performed for the compressible flow of air in a small slender tube. Excellent agreement was found between the tests and models for moderate flows, corroborating the accuracy of the tests and the COMSOL k-ε turbulence model for this

geometry. Only at near-choking conditions was there divergence in the results.

A special technique was employed in COMSOL in order to specify inlet mass flow. This is the quantity usually specified in process applications.

Additionally, a 1-D analytical model was constructed which adds insight to the thermodynamic process of compressible flow; with inlet and outlet loss coefficients derived from one COMSOL model, this model also agreed well with the experiments.

7. Acknowledgements

The authors wish to express their appreciation to the Lord Engineering Corporation, Stephen M. Lord, President, for its generous support of this work.

8. Appendix

Table 1: Experimental Data showing Calculations for Pressure Drop Across a Slender Tube (4.2mm)

	P_{Empty} (Pressure Drop Across the Hose + Fitting)			P_{Total} (Pressure Drop Across the Hose + Fitting + Tube)			P_{Tube} (Pressure Drop Across Tube)
Observed Rotameter Reading (SCFH)	Corrected Flow (SCFH)	Corrected Flow (kg/hr)	Observed Pressure (psig)	Corrected Flow (SCFH)	Corrected Flow (kg/hr)	Observed Pressure (psig)	Calculated Pressure (psig)
100	100.14	3.40	0.04	101.72	3.46	0.51	0.47
150	150.41	5.11	0.08	156.10	5.30	1.22	1.14
200	200.95	6.83	0.14	215.90	7.33	2.43	2.29
250	251.86	8.56	0.22	282.12	9.58	4.02	3.8
300	303.15	10.30	0.31	359.42	12.21	6.4	6.09
350	354.85	12.05	0.41	448.14	15.22	9.4	8.99
400	407.15	13.83	0.53	561.82	19.08	14.3	13.77